Catalysis Science & Technology

PAPER

View Article Online
View Journal | View Issue

Cite this: *Catal. Sci. Technol.*, 2014, **4**, 2340

Vapor phase hydrodeoxygenation of furfural to 2-methylfuran on molybdenum carbide catalysts†

Wen-Sheng Lee,[ac] Zhenshu Wang,[ac] Weiqing Zheng,[bc] Dionisios G. Vlachos[bc] and Aditya Bhan*[ac]

Received 6th March 2014,
Accepted 3rd May 2014

DOI: 10.1039/c4cy00286e

www.rsc.org/catalysis

Vapor phase hydrodeoxygenation (HDO) of furfural over Mo_2C catalysts at low temperatures (423 K) and ambient pressure showed high/low selectivity to C═O bond/C–C bond cleavage, resulting in selectivity to 2-methylfuran (2MF) and furan of ~50–60% and <1%, respectively. Efficient usage of H_2 for deoxygenation, instead of unwanted sequential hydrogenation, was evidenced by the low selectivity to 2-methyltetrahydrofuran. The apparent activation energy and H_2 order for 2MF production rates were both found to be invariant with furfural conversion caused by catalyst deactivation, suggesting that (1) the measured reaction kinetics are not influenced by the products of furfural HDO and (2) the loss of active sites, presumably by formation of carbonaceous species observed by TEM analysis, is the reason for the observed catalyst deactivation. The observed half order dependence of 2MF production rates on H_2 pressure at different furfural pressures (~0.12–0.96 kPa) and the 0–0.3 order dependence in furfural pressure support the idea of two distinct sites required for vapor phase furfural HDO reactions on Mo_2C catalysts. The invariance of 2MF production rates normalized by the number of catalytic centers assessed *via ex situ* CO chemisorption suggests that metal-like sites on Mo_2C catalysts are involved in selective HDO reactions.

1. Introduction

In light of environmental concerns, there has been increasing interest in converting biomass, a renewable alternative energy source, to fuels and chemicals.[1–5] Furfural, considered to be a promising platform molecule derived from the hemicellulosic fraction of lignocellulosic biomass, can produce 2-methylfuran (2MF), furfuryl alcohol, tetrahydrofuran, and tetrahydrofurfuryl alcohol *via* selective deoxygenation and/or hydrogenation.[1,4,6] The conversion of furfural to 2MF, which requires selective removal of the oxygen from the C═O side group of the furan, is of particular interest for fuel production because 2MF has been found to be a promising fuel additive in a practical road trial (high octane number, RON ~131, and low water solubility).[4,7] This process can be achieved by co-feeding hydrogen to remove the oxygen as water; however, this is challenging because, as shown in Scheme 1, hydrogen can, instead of catalyzing selective hydrodeoxygenation (HDO) to give 2MF, hydrogenate the C═O bond to give furfuryl alcohol. Additionally, hydrogenolysis of the C–C bond can occur to give furan and CO, resulting in reduction of the carbon chain length. Unnecessary hydrogen consumption *via* hydrogenation of the furan ring can convert 2MF to 2-methyltetrahydrofuran. Therefore, a critical challenge in converting furfural to 2MF is to selectively cleave the carbonyl oxygen without concurrent successive hydrogenation reactions.

The general trend observed for vapor phase reactions involving furfural and H_2 using Cu, Ni, and Pt based catalysts is that hydrogenation dominates at lower reaction temperatures (<473 K), giving furfuryl alcohol as the major product.[6,8–15] At higher reaction temperatures (>473 K), either sequential hydrogenation reactions are promoted to convert furfuryl alcohol to 2MF[6,9,10,13,16] or decarbonylation of furfural occurs to give furan as the dominant product.[13,17–19] Selectivity to furfuryl alcohol was found to be >90% at low reaction temperatures (≤473 K) for Cu based catalysts, and the selectivity to 2MF increased at the expense of furfuryl alcohol when the reaction temperature increased resulting in a 2MF selectivity of ~50–60% at 573 K.[6,9,14] Pd based formulations catalyze decarbonylation of furfural to give furan as the dominant product at a reaction temperature of 430–600 K, resulting in a 2MF selectivity lower than 20%.[17,19] The selectivity to hydrogenation and decarbonylation pathways was

[a] *Department of Chemical Engineering and Materials Science, University of Minnesota, Minneapolis, MN 55455, USA. E-mail: abhan@umn.edu; Fax: +1 612 626 7246*
[b] *Department of Chemical and Biomolecular Engineering, University of Delaware, Newark, DE, 19716, USA*
[c] *Catalysis Center for Energy Innovation, USA*

† Electronic supplementary information (ESI) available. See DOI: 10.1039/c4cy00286e

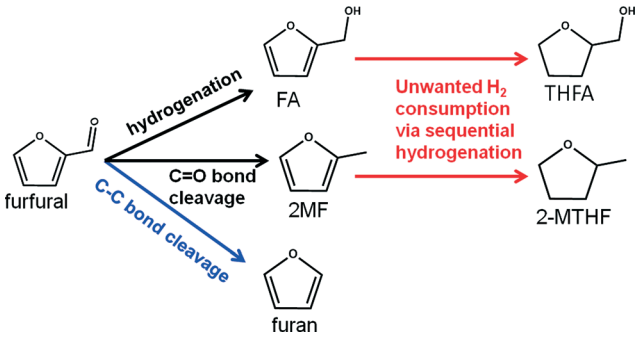

Scheme 1 Possible reaction pathways for furfural conversion in the presence of H_2. FA: furfuryl alcohol, 2MF: 2-methylfuran, THFA: tetrahydrofuran, 2-MTHF: 2-methyltetrahydrofuran.

reported to be dependent on the size and shape of metal particles, types of support used, and the reaction conditions for Pt based catalysts.[8] The presence of promoters and reaction conditions have also been shown to affect the aforementioned reaction pathways for Ni and Pd based catalysts.[11,19]

Recently, transition metal carbides have been reported as an emerging hydrodeoxygenation (HDO) catalyst in which selective removal of oxygen from C_2–C_3 oxygenates,[20,21] vegetable oils,[22] stearic acid,[23] and guaiacol[24] was demonstrated. Herein, we report that molybdenum carbide can accomplish selective C=O bond cleavage, converting furfural to 2MF with a selectivity of ~50–60% in the vapor phase at unprecedentedly low reaction temperatures (~423 K). A very low selectivity to furan (<1%) suggests that unwanted C–C bond cleavage *via* hydrogenolysis is suppressed. Efficient hydrogen usage was inferred from undetectable amounts of 2-methyltetrahydrofuran, a successive hydrogenation product of 2MF. A set of detailed kinetic studies was carried out to reveal plausible reaction mechanisms in which two distinct catalytic sites are involved. Metal-like sites on Mo_2C catalysts are involved in selective HDO as inferred from the near invariance in 2MF production rates normalized by the number of CO adsorption centers, although the requirement of carbidic or oxycarbidic sites for HDO chemistry remains ambiguous at this point.

2. Experimental methods

2.1 Catalyst preparation

Mo_2C catalysts were prepared by a temperature programmed reaction method based on prior reports.[20,25] Typically ~0.6 g of ammonium molybdate tetrahydrate (sieved, 40–80 mesh size, $(NH_4)_6Mo_7O_{24}{\cdot}4H_2O$, Sigma, 99.98%, trace metal basis) was loaded in a tubular quartz reactor with an inner diameter of 10 mm. A total flow rate of ~2.93 $cm^3\ s^{-1}$, consisting of 15/85 vol% of CH_4 (Matheson, 99.97%) and H_2 (Minneapolis Oxygen, 99.999%), was passed through the reactor. The reactor was first heated up in a three-zone split tube furnace (Series 3210, Applied Test System) to ~623 ± 9 K from room temperature (hereafter denoted as RT) with a ramping rate of ~0.06 K s^{-1} and held at that temperature for 12 h; subsequently, the temperature was increased from ~623 ± 9 K to ~873 ± 6 K with a ramping rate of ~0.046 K s^{-1} and the temperature was held constant at 873 ± 6 K for 2 h. The resulting material was then cooled down to RT in the CH_4–H_2 gas mixture for ~3–4 h and subsequently treated in a flowing 1% O_2–He mixture (Matheson, Certified Standard Purity) at ~1.67–3.33 $cm^3\ s^{-1}$ for at least 2 h before being removed from the reactor to prevent the pyrophoric oxidation of the carburized material upon exposure to air.[26] It has been reported that carbon deposition and the number of CO adsorption sites can be sensitive to the carburization conditions.[27,28] As a result, multiple batches of Mo_2C were synthesized and mixed to create representative Mo_2C catalysts without variations caused by using different batches. The first batch of freshly made, passivated Mo_2C samples was stored in a vial (ambient conditions) and then exposed to air when mixed with a second batch of freshly made (and passivated) samples. This mixing process was continued until a total of 12 batches of samples were mixed (labeled as sample A in Table 1). Similar preparation conditions with a <10 K difference in temperature control was used to prepare another representative mixing sample, which contains a total of 15 batches of samples (sample B in Table 1). The mixed Mo_2C samples were stored in a vial (ambient conditions) and aged for <50 days prior to the kinetic measurements and characterization discussed below.

Mo_2C catalysts with varying number of CO adsorption sites were obtained using the aforementioned typical preparation protocol at different temperatures, CH_4/H_2 (vol%) ratios, and flow rate conditions. For example, a protocol for the synthesis of a Mo_2C catalyst with CO chemisorption of ~50 μmol g^{-1} at 323 K (sample #1 in Table 2), "CH_4/H_2-RT (1.5 h)–623 K [24 h] (1.5 h)–873 K [6 h]–cool", represents that the ammonium molybdate tetrahydrate in the reactor was exposed to a gas environment comprising of a CH_4–H_2 mixture and heated up to 623 K within 1.5 h and held at 623 K for 24 h. After that, the temperature was increased to 873 K within 1.5 h and held at 873 K for 6 h before cooling down to RT. Detailed preparation conditions for Mo_2C samples with varying number of CO adsorption sites are listed in Table 2.

2.2 Characterization of molybdenum carbide

X-ray diffraction analysis was performed using a Bruker D8 Discover 2D X-ray diffractometer with a two-dimensional VÅNTEC-500 detector, Cu K_α X-ray radiation with a graphite monochromator, and a 0.5 mm point collimator to identify the bulk structure of the Mo_2C catalysts. The sample was drop casted on a SiO_2 zero-background holder. Three frames at 30° (2θ), 60° (2θ) and 90° (2θ) with a 600 s $frame^{-1}$ dwell ($\Delta 2\theta$ frame width of 35° (2θ)) were measured, and the two-dimensional images were converted to one-dimensional intensity *vs.* 2θ for analysis. The particle size, particle morphology, and the crystal structure of the Mo_2C catalyst were

Table 1 Physical and chemical properties of Mo_2C catalysts and their catalytic performance in a vapor phase furfural HDO reaction

Catalyst[a]	Conditions (prior to characterization)	CO uptake (μmol g^{-1}, STP) 323 K	CO uptake (μmol g^{-1}, STP) 423 K	BET surface area (m^2 g^{-1})	Micropore surface area[e] (m^2 g^{-1})	Mesopore diameter[f] (nm)	Pore volume[g] (cm^3 g^{-1})	Micropore volume[h] ($\times 10^{-3}$ cm^3 g^{-1})	2MF production rate[i] ($\times 10^{-8}$ mol s^{-1} g_{cat}^{-1})	2MF STY[i] ($\times 10^{-5}$ mol s^{-1} mol_{COsite}^{-1})
A	Before reaction[b]	162	50 ± 3.2[j]	24.3[k]	17.1[k]	24 (9.5)	0.042	8.6[k]	1.1	6.5
B	Before reaction[b]	130[j]	31 ± 5.9[j]	18.2[l]	8.8[l]	21 (12)	0.047	4.4[l]	0.63	4.9
A	After reaction[c]	ND	ND	3.3	0.6	40.2 (21.9)	0.018	0.3	N/A	N/A
A	After reaction and chemisorption[d]	306	ND	64.7	55.3	17.9 (8.2)	0.077	27	2.0	6.4
C	Before reaction[b]	250	ND	116.5	78.7	10 (6.4)	0.14	39	ND	ND

[a] Samples A, B, and C were prepared using typical synthesis conditions similar to that for sample #4 in Table 2. [b] Samples A, B, and C were exposed to air and aged in a vial for 41 days, 17 days and <1 (freshly made) day, respectively, prior to CO chemisorption and N_2 adsorption measurements. [c] The catalyst was, instead of treating in a flow of 1% O_2 in He, cooled down from reaction temperature (~423 K) to RT in the reactant mixture and then removed from the reactor prior to N_2 adsorption measurement. [d] The spent sample was pretreated in H_2 at 723 K for 2 h prior to CO chemisorption measurement. After chemisorption, the sample was passivated in a flow of 1% O_2 in He at RT for at least 2 h prior to N_2 adsorption measurements. [e] Estimated from the *t*-plot method. [f] Estimated from the BJH adsorption branch (BJH desorption branch). [g] Estimated at the relative pressure $P/P_0 = 0.98$. [h] Estimated from the *t*-plot method. [i] Calculated as an average value between 8 and 9 h time-on-stream with a furfural conversion of ~7% (see discussion in reference to Fig. 4) and normalized by the amount of irreversibly chemisorbed CO measured at 323 K; catalysts were activated in a flow of H_2 (~1.67 cm^3 s^{-1}) at ~750 K for 1 h prior to kinetic measurements. [j] Reported as the average value of independent repeated measurements at different aging times shown in Fig. 3(b). Detailed data are listed in Table S1 in the ESI. [k] Data reported as the average value of three independent N_2 adsorption measurements shown in Fig. 3(a). Complete data set presented in Table S2 in the ESI. [l] Data reported as the average value of two independent N_2 adsorption measurements (not shown in Fig. 3(b)) and the corresponding data set is presented in Table S2 in the ESI. ND: not determined.

Table 2 Preparation conditions for high surface area Mo_2C samples with varying numbers of catalytic centers measured by CO chemisorption at 323 K

Catalyst[a]	AMT[b] (g)	CH_4 flow rate (cm^3 s^{-1})	H_2 flow rate (cm^3 s^{-1})	Temp profile[c]	CO chemisorption uptake (μmol g^{-1}, STP) at 323 K
#1	3.0	0.4	0.7	CH_4/H_2-RT (1.5 h)–623 K [24 h] (1.5 h)–873 K [6 h]–cool	51
#2	6.0	0.4	2.5	H_2-RT (1.5 h)–618 K [15 h]–CH_4/H_2 (1.5 h)–863 K [2 h]–cool	119
#3	0.6	0.4	2.5	CH_4/H_2-RT (1.5 h)–623 K [12 h] (1.5 h)–873 K [2 h]–cool	127
#4	0.6	0.4	2.5	CH_4/H_2-RT (1.5 h)–623 K [12 h] (1.5 h)–873 K [2 h]–cool	135
#5	0.6	0.4	2.5	CH_4/H_2-RT (1.5 h)–623 K [12 h] (1.5 h)–863 K [2 h]–cool	138
#6	3.6	0.4	2.5	CH_4/H_2-RT (1.5 h)–623 K [12 h] (1.5 h)–858 K [4 h]–cool	139
#7	2.2	0.4	2.5	CH_4/H_2-RT (1.5 h)–623 K [14 h] (1.5 h)–848 K [3 h]–cool	201
#8	1.0	0.4	2.5	CH_4/H_2-RT (1.5 h)–608 K [12 h] (1.5 h)–843 K [2 h]–cool	231

[a] Samples #7 and #8 were freshly made and the corresponding CO chemisorption and kinetic measurements were carried out within 2 days of Mo_2C synthesis. The rest of the samples were aged for <1 month but the CO chemisorption was re-measured within 2 days of the kinetic measurements for those samples. [b] Ammonium molybdate tetrahydrate (sieved, 177–400 μm). [c] Detailed description for the preparation conditions can be found in section 2.1. For the catalysts prepared by heating in a pure H_2 environment first, such as sample #2 (H_2-RT (1.5 h)–618 K [15 h]–CH_4/H_2 (1.5 h)–863 K [2 h]–cool), the switch of H_2 to CH_4/H_2 was achieved by adding CH_4 (0.44 cm^3 s^{-1}) to the existing H_2 flow (2.49 cm^3 s^{-1}).

characterized *via* transmission electron microscopy (TEM JEOL JEM-2010F, 200 kV). For TEM sample preparation, the Mo_2C catalyst was ground and acetone was added to make a suspended solution in an ultrasonic bath. A drop of solution was placed onto a holey-carbon coated Cu grid and dried in air under ambient conditions prior to TEM analysis. The BET/micropore surface area, pore/micropore volume, and mesopore size were measured *via* N_2 physisorption using a Micromeritics ASAP 2020 analyzer. Before these measurements, the fresh, passivated sample and the spent sample were degassed (<6 μm Hg) at 523 K and RT, respectively, for at least 4 h. CO (Matheson, 99.5%) chemisorption uptakes were measured at either 323 K or 423 K using a Micromeritics ASAP 2020 analyzer. Prior to these measurements, the samples were evacuated at 383 K (~2 μm Hg) for 0.5 h and then treated in H_2 at 723 K for 2 h, followed by degassing (~2 μm Hg) at 723 K for 2 h before the first adsorption isotherm measurement (between 100 and 450 mm Hg) at either 323 K or 423 K. The catalysts were then degassed (~2 μm Hg) to remove weakly adsorbed species prior to measurement of the second isotherm. Both isotherms were extrapolated to zero pressure and the difference between the two extrapolated values was assessed as the amount of irreversibly adsorbed CO.[28]

2.3 Kinetic measurements of vapor phase furfural hydrodeoxygenation (HDO)

Vapor phase HDO of furfural was carried out in a flow through quartz reactor (10 mm inner diameter), at atmospheric pressure, housed within a three-zone split tube furnace (Series 3210, Applied Test System) controlled by three temperature controllers (Watlow, EZ-zone) and using ~0.02–0.64 g Mo_2C catalyst of 40–80 mesh size. The typical reaction temperature was ~423 K and was monitored by attaching a type K thermocouple to the bottom of a well on the external surface of the quartz reactor. The typical pressure drop caused by the catalyst bed was <3 kPa. Prior to the measurement of reaction rates, the catalyst was treated in H_2 (Minneapolis Oxygen, 99.999%) with a total flow rate of ~1.67 $cm^3\ s^{-1}$ at ~750 ± 10 K for 1 h (with a ramping rate of ~0.19 K s^{-1} from RT). Subsequently, the reactor temperature was cooled to ~423 K and the gas flow was switched from pure H_2 to the reaction mixture (~1.67 $cm^3\ s^{-1}$) consisting of ~0.24%/2.5%/bal of furfural (Sigma, 99% ACS reagent), CH_4 (Matheson, 99.97%), and H_2 (Minneapolis Oxygen, 99.999%) in which CH_4 was used as an internal standard. Furfural was further purified *via* vacuum distillation prior to being fed in the flowing gas stream (H_2–CH_4 mixture) with a syringe pump (KD Scientific, Model 100) equipped with a gas tight syringe (SGE Analytic Science). All flow lines were heated to at least 373 K *via* resistive heating to prevent condensation of effluents. The reactor effluent was analyzed using an Agilent 6890 gas chromatograph outfitted with an automatic sampling valve and two sample loops. Organic products were separated using a methyl-siloxane capillary column (HP-1, 50 m × 320 μm × 0.52 μm) and analyzed *via* a flame ionization detector (FID). The FID response factors (RF) for the identified products were obtained by calibrating the GC with known compositions of the corresponding reference reagents, while the quantification of unidentified heavier compounds was estimated by using a measured RF of decane. Permanent gases (H_2 and CO) were separated by a Supelco HAYSEP DB packed column (1/8 in. × 12 ft) and analyzed by a thermal conductivity detector (TCD). The carbon balance was typically better than 95% and the error associated with the quantification for furfural was found to be around 4%. The mass balance, furfural conversion, and product selectivity are based on a carbon basis and are defined as follows:

$$\text{Mass balance} = \frac{\text{(moles of C measured from the reactor effluent)}}{\text{(moles of C in the feed)}}$$

$$\text{Furfural conversion} = \frac{\text{(sum of the carbon in products)}_{out}}{\text{(moles of carbon in furfural)}_{in}}$$

$$\text{Product selectivity} = \frac{\text{(moles of carbon in product i)}}{\text{(the sum of carbon in products)}}$$

The calculations above are based on the measured eluent concentration by GC and any potential errors associated with coke formation during catalysis are not included.

Furfural conversion was controlled to be <15% for the kinetic studies. Mears' criteria were employed to confirm the absence of external heat and mass transfer limitations (Table S3, ESI†). Internal mass transfer limitations were negligible because the estimated Thiele modulus was much smaller than 1 (Table S4, ESI†).

3. Results and discussion

3.1 Characterization of molybdenum carbide catalysts

Bulk carburization was achieved as evidenced by the absence of peaks assigned to either MoO_2 or MoO_3 in the XRD pattern for a representative fresh Mo_2C catalyst (sample A, Table 1), as shown in Fig. 1. The structural phase of Mo_2C was found to be primarily β-Mo_2C (Joint Committee on Powder Diffraction Standards, no. 35-0787, 2θ peaks at ~34.355° (100), 37.979° (002), 39.393° (101), 52.124° (102), 61.529° (110), 69.567° (103), 74.647° (112), and 75.514° (201)) with a minor presence of α-Mo_xC_{1-x} (Joint Committee on Powder Diffraction Standards, no. 15-0457, 2θ peaks at ~37.768° (111), 43.693° (200), 63.396° (220), 75.727° (311), and 79.869° (222)) based on the comparison of the major peak intensities from those two phases. Since both β-Mo_2C and α-Mo_xC_{1-x} have a Mo to C molar ratio of ~2, the catalysts used in this work are therefore denoted as Mo_2C. The presence of β-Mo_2C in a representative fresh Mo_2C catalyst (sample A, Table 1) was also confirmed by lattice indexing using HRTEM images. Lattice fringes and the analysis of their characteristic acute angles indicate the existence of hexagonal close packed β-Mo_2C in both fresh and spent catalysts, as shown in Fig. 2. The Mo_2C prepared in this work was inferred to be polycrystalline because of the arrangement of discrete spots observed in the selected area electron diffraction (SAED) of a typical Mo_2C

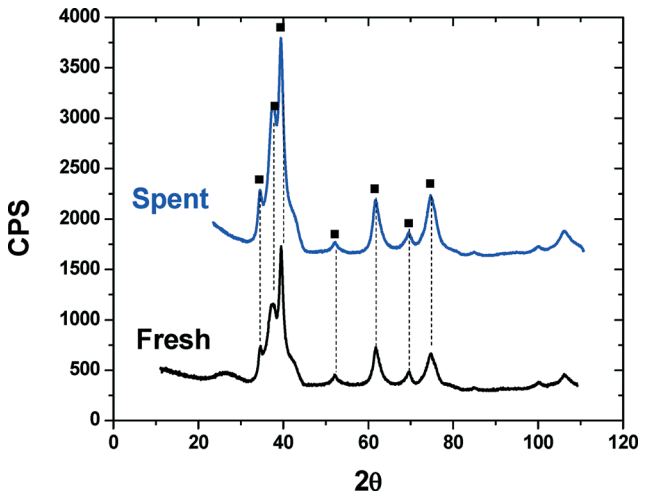

Fig. 1 X-ray diffraction patterns of fresh and spent Mo_2C catalysts after kinetic measurements shown in Fig. 4 (sample A in Table 1). The fresh sample was treated in a flowing 1% O_2–He mixture (~1.67–3.33 $cm^3\ s^{-1}$) for at least 2 h at RT and the spent sample was cooled down from reaction temperature (~423 K) to RT in the reactant mixture (furfural/CH_4/H_2 = ~0.24%/2.5%/bal, total flow rate ~1.67 $cm^3\ s^{-1}$) prior to XRD measurement.

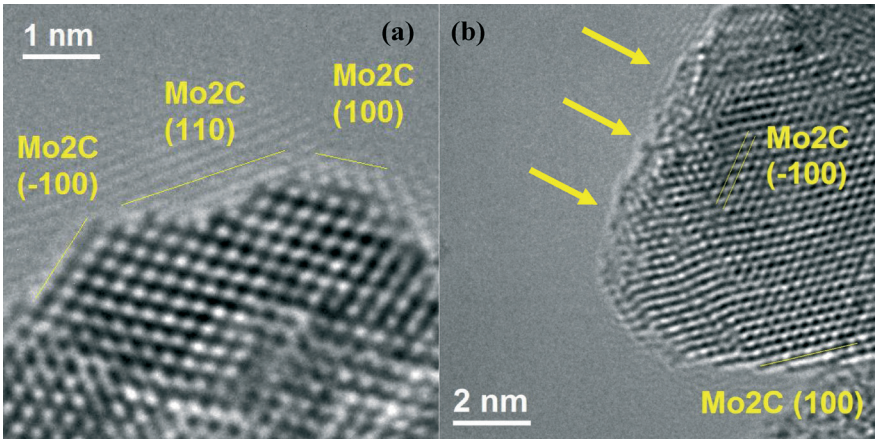

Fig. 2 Representative HRTEM images of (a) fresh, passivated and (b) spent Mo_2C catalysts after kinetic measurements shown in Fig. 4 (sample A in Table 1) in which different crystal planes of β-Mo_2C were identified. Thick layers of carbon species (indicated by arrows) were observed in the spent sample.

particle (Fig. S1(b) in the ESI†). The porous features of Mo_2C were evidenced by the existence of a hysteresis loop at relative pressures (P/P_0) of ~0.3 to 0.6 in a N_2 adsorption experiment (Fig. S2 in the ESI†).

Fig. 3(a) shows BET surface area and pore volume of Mo_2C samples exposed to air and aged for different periods of time in which a significant loss in the BET surface area and pore volume was observed for the freshly made sample (single batch without mixing with other batches of Mo_2C samples, sample C in Table 1). Sample C in Table 1, passivated in a flow of 1% O_2 in He prior to being stored in a vial, was inevitably exposed to air each time prior to CO chemisorption and N_2 physisorption measurements and there were a total of 7 (4 physisorption and 3 chemisorption) measurements in 11 days. Since molybdenum oxide has much lower surface area (~1 $m^2\ g^{-1}$) than molybdenum carbide and sample exposure to air was the only event that occurred during characterization, the significant reduction in the BET surface area and pore volume for sample C could potentially be caused by oxidation even after the sample was passivated as per the procedure recommended by Boudart and coworkers.[28] Leary *et al.*[29] reported that a Mo_2C sample can incorporate ~2 monolayers of oxygen upon exposure to air at room temperature by TPR experiments and that a passivation step cannot prevent additional oxygen uptake. The amount of oxygen or the time that the samples were exposed to air would be a more apposite descriptor instead of the shelf time shown in Fig. 3; however, these data qualitatively show that a Mo_2C sample, even after passivation, will have a noticeable reduction in both surface area and pore volume, presumably caused by oxidation under ambient conditions.

A noticeable loss in CO uptake in chemisorption experiments for the freshly made sample (sample C, Table 1) was also observed as a function of aging time (Fig. 3(b)). This experimental result suggests that some catalytic sites were irreversibly lost, presumably by oxidation, during the aging process, which could not be recovered by the H_2 treatment (723 K, 1 h) carried out prior to CO chemisorption. The catalytic centers titrated by CO chemisorption were found to track with the measured BET surface area for the freshly made sample (sample C, Table 1), as shown in Fig. 3(a) and (b); this correlation of CO chemisorption and BET surface area is consistent with the data reported by Ranhotra *et al.*[30] and Lee *et al.*[28]

Samples comprising multiple batches of Mo_2C formulations (samples A and B in Table 1) showed relatively stable BET surface areas (Fig. 3(a)) and CO chemisorption (Fig. 3(b)) in contrast to a freshly prepared Mo_2C sample (sample C, Table 1). The slight difference in CO chemisorption uptake for samples A and B may be attributed to the slight variations in the preparation temperature mentioned in section 2.1. During the preparation of samples A and B, the different Mo_2C batches were exposed to air each time upon mixing, and therefore, the BET surface area and CO uptake in chemisorption (measured at either 323 or 423 K) had already decreased and reached stable values prior to the characterization measurements. This experimental result suggests that there are at least two types of catalytic centers which can be titrated by CO: one (hereafter denoted as type A) that can be lost during the aging process (presumably due to oxidation) and cannot be recovered by H_2 treatment (723 K, 1 h) as illustrated by the decrease in the CO chemisorption uptake for sample C as a function of time (Fig. 3(b)) and the other one (hereafter denoted as type B) that was either unaffected by the aging process or capable of being regenerated by the H_2 treatment. No indication of bulk MoO_3 and/or MoO_2 was found for the representative aged Mo_2C sample (sample A, Table 1) for which a significant loss in the BET surface area and pore volume was observed during the aging process.

Samples A and B listed in Table 1, unless otherwise mentioned, were used for kinetic studies because of their stable CO uptake in chemisorption measurements. 2MF site time yield (hereafter denoted as 2MF STY) was calculated by normalizing the 2MF production rate per catalytic

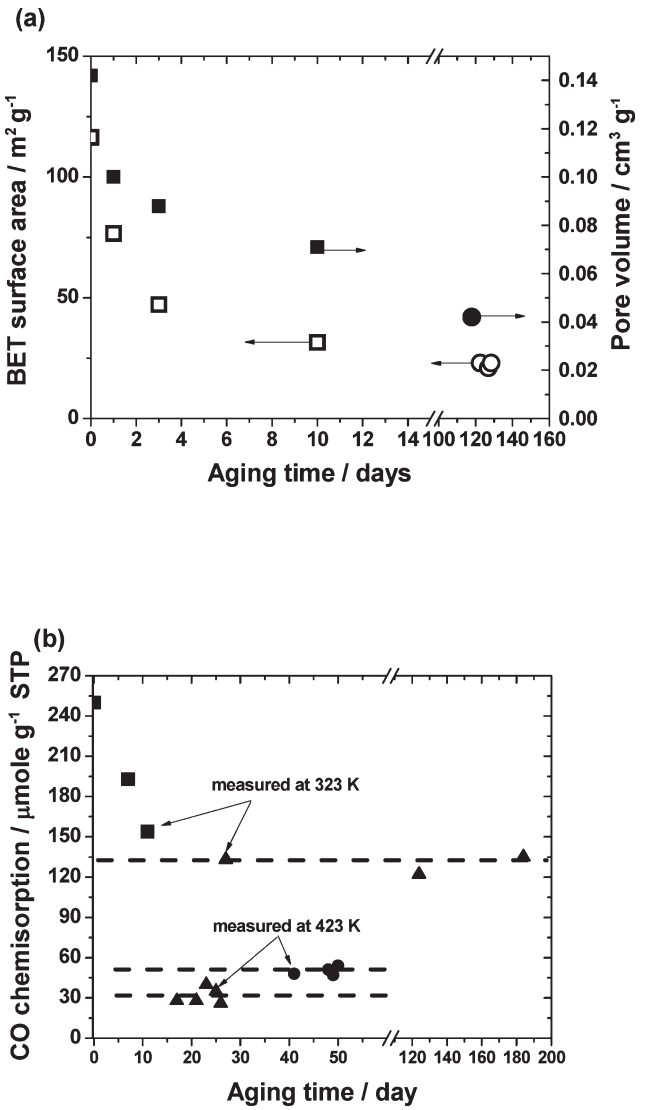

Fig. 3 (a) Evolution of BET surface area (□ for sample C and ○ for sample A in Table 1) and pore volume (■ for sample C and ● for sample A in Table 1) as a function of aging time. (b) CO chemisorption for Mo_2C samples (sample A (●) and sample B (▲) in Table 1) exposed to air, stored in a vial and aged for >15 days and for a freshly made sample (sample C (■) in Table 1) aged <15 days. The dashed line is drawn to guide the eye.

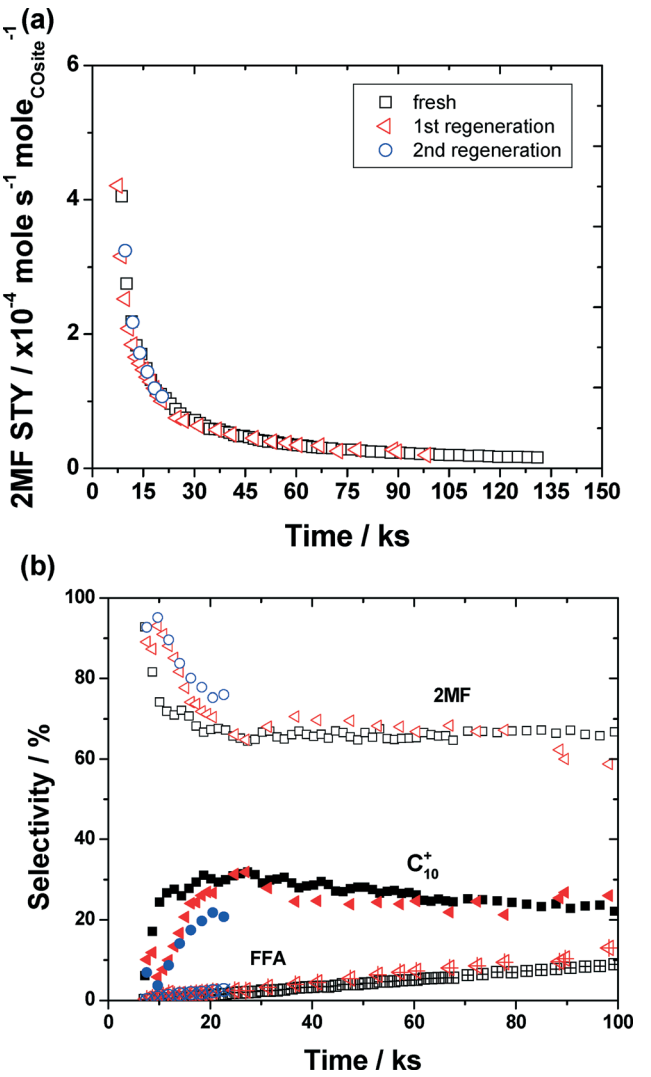

Fig. 4 (a) 2-Methylfuran site time yield (2MF STY). (b) Furfural hydrodeoxygenation product selectivity (2-methylfuran (2MF), C_{10}^+, and furfuryl alcohol (FA)). Fresh Mo_2C catalyst (□, ■, ⊞) and the same catalyst after the first (◁,◀,⧓) and second (○, ●, ⊠) regeneration cycle. Reaction conditions: furfural/CH_4/H_2 = ~0.24%/2.5%/bal (total flow rate ~1.67 cm^3 s^{-1}), reaction temperature ~423 K under ambient pressure. The kinetic data of Mo_2C catalysts for vapor phase furfural HDO was first reported by Xiong *et al.*,[25] it has been re-plotted in this work.

center measured by CO chemisorption at either 323 K (Table 1) or 423 K.

3.2 Catalytic performance of molybdenum carbide catalysts for vapor phase furfural HDO

Fig. 4 shows 2MF STY normalized by CO chemisorption measured at 323 K and product selectivity as a function of time for vapor phase furfural HDO on Mo_2C catalysts (sample A in Table 1), which has also been reported in our previous work.[25] Mo_2C catalysts suffered from deactivation, which is similar to what has been observed for the same reaction using Cu/C and copper chromite catalysts.[9,15] The reaction rate did not reach a steady state even after 20 h time-on-stream. The reaction, however, is catalytic because the estimated turnover number of ~22 (calculated as the 2MF yield between 5.7 and 131 ks time-on-stream, which is ~0.0011 mol g_{Cat}^{-1}, divided by the amount of irreversibly chemisorbed CO measured at 423 K (~50 μmol g_{Cat}^{-1})) was much larger than 1.[25]

2MF was found to be the dominant product with a selectivity of ~50–60% at all times-on-stream as shown in Fig. 4(b). The second major product was C_{10}^+ compounds with a selectivity of ~30%. The data reported in Fig. 4(b) show that 2MF and C_{10}^+ selectivities vary with time-on-stream up to 25 ks, suggesting that the surface of the Mo_2C catalyst was evolving. The selectivities to 2MF and C_{10}^+ were, however, nearly invariant (2MF selectivity of ~60% and C_{10}^+ selectivity of ~30%, Fig. 4(b)) after 25 ks, suggesting that no preferential

loss of sites for 2MF production occurred in the subsequent time period. The selectivity to furan, the product of C–C bond cleavage from furfural, was less than 1%, which was also commensurate with the amount of CO measured within stoichiometric error (furfural → furan + CO), suggesting that Mo_2C can very selectively break C═O bonds instead of the C–C bond. The high 2MF selectivity (~50–60%) and low furan selectivity (<1%) at relatively low reaction temperatures (~423 K) and atmospheric pressure distinguish Mo_2C formulations from Cu, Pd, and Ni catalysts for furfural HDO.[13] For example, furfuryl alcohol was the primary product over several copper based catalysts at reaction temperatures less than 473 K, while 2MF became the dominant product only for reaction temperatures higher than ~523 K.[9,31] Palladium catalysts were found to preferentially break the C–C bond of furfural, giving furan as the dominant product at reaction temperatures in the range of 483 to 523 K.[12,13] It has been reported recently that both furfuryl alcohol and furan are primary products for monometallic Ni catalysts; however, 2MF selectivity can be greatly enhanced by addition of Fe to form Ni–Fe bimetallic compositions.[11] The highest 2MF selectivity observed for the SiO_2 supported Ni–Fe bimetallic catalysts with 5 wt% Ni–5 wt% Fe formulation was found to be ~65% at 523 K and 1 atm, which is slightly higher than the 2MF selectivity observed for the Mo_2C catalyst tested at ~423 K in this study.

A GC-MS analysis of the reactor effluents showed C_{10}^+ products such as decane and 2-(furan-2-ylmethyl)-5-methylfuran, a dimerization product of 2MF. The C_{10}^+ compounds can, presumably, be produced by dimerization of furfural and/or furfuryl alcohol *via* acid-catalyzed reactions[32–34] followed by sequential deoxygenation reactions. The existence of acidic sites on Mo_2C catalysts has been shown by probe reaction studies and NH_3 temperature programmed desorption experiments.[35]

Fig. 5 shows the selectivity of 2MF and furfuryl alcohol as a function of furfural conversion, which was obtained by either using different amounts of catalysts (solid symbols (●, ■), data reported as the average value of 2–3 h time-on-stream, sample A, Table 1) or plotting the selectivity data of a sample deactivating with time on stream starting at a furfural conversion of ~12% (open symbols (○, □), sample A, Table 1). The data obtained from those two different methods were found to be superimposable, suggesting that the change in the number, not the identity or reactivity, of the active sites is the reason for catalyst deactivation. A low BET surface area was found for the spent catalyst (~3.3 $m^2\ g^{-1}$), as compared to that for the same sample after CO chemisorption (~65 $m^2\ g^{-1}$), as shown in Table 1. There are two possibilities that account for catalyst deactivation: (1) the formation of carbonaceous species, which could possibly block the pores and prevent the reactants from accessing the active sites inside the pores, and (2) oxidation of the carbidic phase to an oxide or oxycarbide phase due to the presence of oxygenates (reactants), which presumably is the cause for the loss of BET surface area (and therefore numbers of catalytic

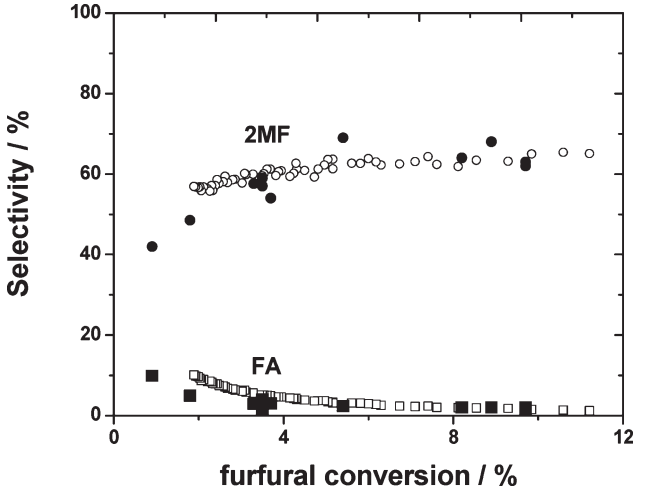

Fig. 5 2-Methylfuran (2MF) and furfuryl alcohol (FA) selectivities as a function of furfural conversion. Data were obtained by (1) using different amounts of catalyst (●, ■) (sample A in Table 1, 0.02–0.3 g) and taking the average value of the kinetics data at 2–3 h time-on-stream and (2) catalyst deactivation for the same catalyst (□, ○) (sample A in Table 1) starting from a high furfural conversion of ~12%.

centers measured by CO chemisorption) as discussed above. While this study does not focus on discerning the contribution of each factor to the catalyst deactivation, coke formation was evidenced by TEM analysis. A layer of amorphous species on a representative spent Mo_2C particle (sample A, Table 1) was observed in the HRTEM image (indicated by an arrow in Fig. 2(b)). A clear reconstruction of the surface in a spent Mo_2C particle was observed when it was exposed to a high energy electron beam (see movie in the ESI†) and this amorphous surface species, only observed on the spent Mo_2C catalyst, was attributed to the formation of carbonaceous species during the reaction because the lighter carbonaceous species, as compared to the neighboring heavier molybdenum atoms, can be easily excited by the electron beam.

Because catalyst deactivation was attributed to the loss of the active sites, we chose the average kinetic data between 8 and 9 h time-on-stream shown in Fig. 4(a) (with a furfural conversion of <10% and corresponding to ~14 turnovers based on the amount of irreversibly chemisorbed CO measured at 423 K, ~50 $\mu mol\ g_{Cat}^{-1}$), as a reference to quantitatively compare the rate of C═O bond cleavage and that for C–C bond scission. The 2MF STY (normalized by the amount of irreversibly chemisorbed CO on the Mo_2C at 323 K, ~6.5×10^{-5} mol s^{-1} mol_{COsite}^{-1}) was found to be two orders of magnitude higher than the furan STY (~0.4×10^{-6} mol s^{-1} mol_{COsite}^{-1}) calculated under the same conditions, which clearly demonstrates that the Mo_2C catalyst very selectively cleaves C═O bonds (Fig. 4(a)).

A comparison between Mo_2C catalysts and other catalysts used for 2MF production *via* vapor phase furfural HDO is challenging because (i) the reaction conditions employed vary amongst the different reports, (ii) the rate may change with time-on-stream due to deactivation, (iii) product inhibition, which is not observed for Mo_2C formulations under the

conditions we report, may become relevant, and (iv) the identity of the active sites is not known. An estimation can be made by comparing the specific 2MF production rate per gram of catalyst; however, catalyst deactivation prevents a well-defined reference for rate comparison. A specific 2MF production rate per gram of catalyst with a furfural conversion of ~96% and a 2MF selectivity of ~39% for a Ni–Fe bimetallic catalyst (5 wt% Ni and 2 wt% Fe) reported by Resasco and coworkers[11] is ~1.1×10^{-5} mol s^{-1} g_{Cat}^{-1} at 523 K and 1 atm and that for a Cu–Al alloy estimated from the early work of Bremner and Keeys (with a furfural conversion of >90% and a 2MF selectivity of >80%) was ~3.5×10^{-7} mol s^{-1} g_{Cat}^{-1} at ~523 K.[31] The average 2MF production rate between 2–3 h and 8–9 h time-on-stream for the Mo_2C catalysts extrapolated to 523 K based on the apparent E_a of ~85 kJ mol^{-1} (shown in Fig. 9) was ~9×10^{-6} and ~1×10^{-6} mol s^{-1} g_{Cat}^{-1}. Vannice and coworkers[9] reported a furfural consumption rate of ~1.7×10^{-5} mol s^{-1} g_{Cat}^{-1} at 413 K for copper chromite with a furfuryl alcohol selectivity of ~70%. If we assume that 2MF is the only product other than furfuryl alcohol, the 2MF production rate was found to be ~5×10^{-6} mol s^{-1} g_{Cat}^{-1} at 413 K for the copper chromite catalysts. The average 2MF production rate between 2–3 h and 8–9 h time-on-stream for the Mo_2C catalysts extrapolated to 413 K based on the apparent E_a of ~85 kJ mol^{-1} (shown in Fig. 9) was ~1.9×10^{-8} and ~6.1×10^{-9} mol s^{-1} g_{Cat}^{-1}, respectively.

The furfural conversion and the product selectivities were completely restored by treating the spent catalyst (sample A in Table 1) in a flow of H_2 (~1.67 cm^3 s^{-1}) at ~750 K for 1 h (Fig. 4), which is in accordance with the observation that the type B site categorized by CO chemisorption present in sample A can be fully regenerated by H_2 treatment as discussed in section 3.1. The effect of H_2 treatment on catalyst regeneration also suggests that using a higher H_2 pressure, which is typically used to reduce coke formation for HDO of phenolic compounds[2,36,37] and can also lower the propensity of carbidic sites being oxidized by lowering the oxidizing potential of the reactant stream, will likely alleviate and/or eliminate catalyst deactivation. The catalyst, after the first regeneration, showed slightly higher average 2MF production rates per gram of the catalyst between 8 and 9 h time-on-stream, ~2.0×10^{-8} mol s^{-1} g_{cat}^{-1}, as compared to that for the fresh catalyst, ~1.1×10^{-8} mol s^{-1} g_{Cat}^{-1} (Table 1, a plot of 2MF production rate per gram of catalyst *vs.* time-on-stream is shown in Fig. S3 in the ESI†). The amount of irreversibly chemisorbed CO measured at 323 K for the spent sample (after two consecutive regeneration tests shown in Fig. 4) in which the sample was pretreated in a flow of H_2 at ~723 K for 2 h prior to CO chemisorption was also found to be higher, ~306 μmol g^{-1} (Table 1). The reason for the observed increase in the CO chemisorption uptake for the sample after regeneration might be attributed to the further removal of the residual oxygen in the carbide catalyst when the sample was treated in a flow of H_2.[29,30] If we consider that the number of active sites measured by *ex situ* CO chemisorption for the sample after the second regeneration is the same as that after the first regeneration (because no measurable differences in catalytic rates or selectivity are observed after the first and second regeneration), the 2MF STY normalized by the amount of irreversibly chemisorbed CO measured at 323 K was found to be the same (~6.5×10^{-5} mol s^{-1} mol_{COsite}^{-1}) for the fresh catalyst and the catalyst after regeneration (Table 1). This experimental observation suggests that the 2MF production rates scale with the number of catalytic centers measured by *ex situ* CO chemisorption; this was further confirmed by the invariance of 2MF STY for Mo_2C samples with varying numbers of CO chemisorption sites as discussed in section 3.4 below.

3.3 Kinetics of vapor phase furfural HDO on molybdenum carbide catalysts

Kinetic measurements were carried out after the following issues were addressed: (1) ensuring the reaction is in a kinetically controlled regime, (2) excluding any observable kinetic effects of furfural HDO products on the 2MF production rate, and (3) correcting for catalyst deactivation to assess intrinsic kinetic parameters, such as reaction orders and apparent activation energy. All kinetic studies were conducted under differential conditions (the furfural conversion was <15%). The furfural conversion for sample A in Table 1 was varied between ~1% and ~10% by varying the amount of the catalyst from 0.02 to ~0.32 g and the space velocity from 0.01 to 0.19 cm^3 s^{-1} g_{Cat}^{-1}. The average 2MF STY (normalized by the amount of irreversibly chemisorbed CO at 323 K) either between 2 and 3 h or between 8 and 9 h time-on-stream *versus* furfural conversion is plotted in Fig. 6. The average 2MF STY (2.1 ± 0.3 × 10^{-4} mol s^{-1} mol_{COsite}^{-1} for 2–3 h time-on-stream and 0.62 ± 0.1 × 10^{-4} mol s^{-1} mol_{COsite}^{-1} for 8–9 h time on stream) was invariant over this range of

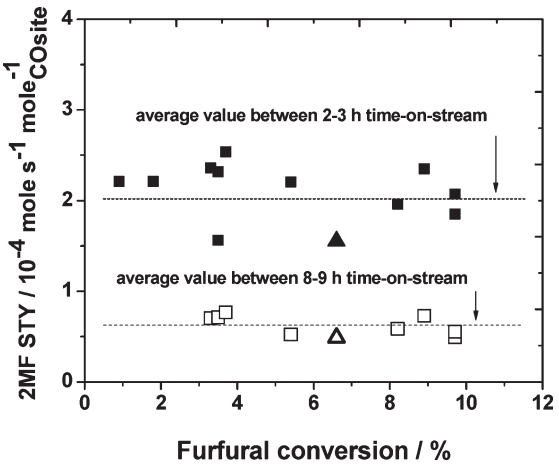

Fig. 6 2-Methylfuran site time yield (2MF STY; normalized by CO chemisorption measured at 323 K, reported as the average value between the specified times on stream indicated in the figure) for Mo_2C samples as a function of furfural conversion achieved using different amounts of catalysts (sample A (■, □) and sample B (▲, △) in Table 1, 0.02–0.32 g). Reaction conditions: furfural/CH_4/H_2 = ~0.24%/2.5%/bal (total flow rate ~1.67 cm^3 s^{-1}); reaction temperature ~423 K under ambient pressure. The dashed lines are drawn to guide the eye.

furfural conversion. This experimental result suggests that there is negligible product inhibition under the current reaction conditions. The effect of catalyst deactivation during the measurement of reaction kinetics was assessed by choosing standard conditions and the corresponding measured 2MF STY as a reference. After each measurement of 2MF STY at a reaction temperature or reactant partial pressure other than the standard conditions, the reaction conditions were restored to the chosen standard conditions and the corresponding 2MF STY was measured. The 2MF STY measured at varying temperature and partial pressure conditions was then corrected by multiplying the ratio of the 2MF STY under the chosen standard conditions experimentally measured at different times-on-stream to account for deactivation. An illustrative example for calculating the apparent H_2 reaction order and apparent activation energy is available in sections 2.3 and 2.4 in the ESI.† Alternatively, one can fit the data measured under the chosen standard conditions to obtain a deactivation curve and use this curve to predict the corresponding 2MF STY at the time-on-stream when the 2MF STY was measured under conditions other than the standard conditions. The extent of catalyst deactivation can then be accounted, similarly, by calculating the ratio of 2MF STY under the chosen standard conditions at different times-on-stream. The two methods of correcting for the catalyst deactivation gave very similar dependence of 2MF STY on H_2 pressure: ~0.56 order (using the experimentally measured 2MF STY) and ~0.51 order (using 2MF STY predicted using the deactivation curve). Detailed information regarding the use of these two different methods to calculate apparent H_2 order can be found in section 2.3 in the ESI† (see Table S5, Fig. S4–S7 and an illustrative example in the ESI†). Since no significant differences between these two methods for assessment of the effects of deactivation on measured kinetics were noted, all kinetic data measured were corrected for catalyst deactivation by re-measuring the 2MF STY under the standard conditions every time.

Fig. 7(a) and (b) show the dependence of 2MF STY on H_2 and furfural pressures (for the sample after two regeneration cycles shown in Fig. 4), respectively, in which the H_2 partial pressure was varied from ~0.1 to ~1 atm (balance He) and the furfural partial pressure was varied from ~0.03 to ~30 kPa at 423 K. The apparent H_2 order was found to be ~0.5, suggesting that dissociative adsorption of hydrogen occurs. The apparent furfural order was found to be ~0.3 at a furfural partial pressure of ~0.03 to ~3 kPa and close to zero at a furfural partial pressure of >10 kPa. The observed zero order in furfural implies that furfural and molecular H_2 do not compete for the same sites, since, otherwise, an inhibition of catalytic rate by furfural would be observed. The apparent H_2 order was found to be independent of the furfural concentration (~6–25 kPa) as shown in Fig. S8 in the ESI,† showing that furfural and H_2 activation requires two distinct sites.

Surface science studies by Ko and coworkers[38,39] have suggested that H_2 is dissociated in four-fold hollow sites on Mo_2C surfaces while CO is adsorbed on on-top sites, thereby establishing a precedent for distinct sites on Mo_2C surfaces. Considering that the 2MF STY correlates with the amounts of CO chemisorption sites available (discussed in section 3.4), we postulate that on-top sites, which are responsible for CO chemisorption, can activate furfural adsorption while a distinct site(s) is used for activating molecular hydrogen.

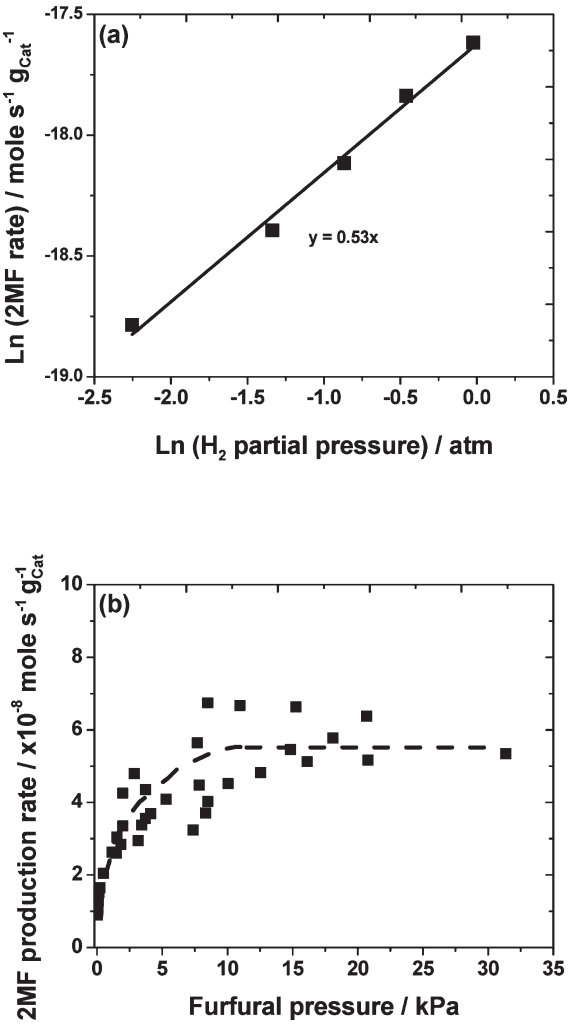

Fig. 7 (a) Effect of H_2 pressure (varied from ~0.1 to ~1 atm (balance He) at ~0.24 kPa furfural at 423 K) and (b) effect of furfural pressure (varied from ~0.03 to ~30 kPa with CH_4 as an internal standard) on 2MF production rate for a typical Mo_2C catalyst (sample A in Table 1). The dashed line is drawn to guide the eye. All the kinetic data were corrected for catalyst deactivation by reference to the chosen standard conditions. Experimental data were obtained at a total pressure of 1 atm.

Fig. 8 shows that the apparent H_2 order for 2MF STY at varying furfural conversion, achieved by deactivation of a catalyst starting from a high furfural conversion (~13%), was ~0.5 and invariant, suggesting that the reaction mechanism and/or the identity of the active sites remains the same as the catalyst deactivates. Similar apparent H_2 orders measured for a sample undergoing the first, second, and third regeneration cycles (Fig. 8) also suggests that the active sites on the Mo_2C catalyst (type B CO chemisorption sites as discussed in

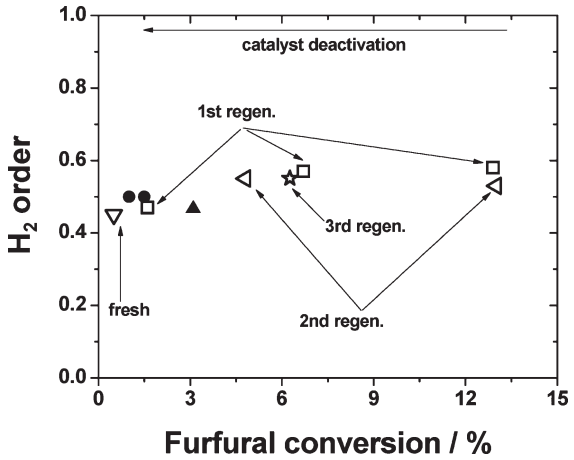

Fig. 8 Apparent H_2 order of 2MF production rates as a function of furfural conversion. Varying concentrations were achieved by using different amounts of Mo_2C catalysts ((●) sample A, (▲) sample B in Table 1, ~0.3–0.64 g) and by catalyst deactivation for the same catalyst (sample A in Table 1) starting from a high furfural conversion of ~13%. H_2 order was found to be independent of catalyst deactivation and catalyst regeneration (▽, □, ◁, and ☆ represent the same catalyst at different states indicated by arrows). Experimental data obtained at 423 K, H_2 pressure varied from ~0.1 to ~1 atm (balance He) at ~0.24 kPa furfural and ~2.5 kPa CH_4 as an internal standard with a total flow rate of ~1.67 $cm^3\ s^{-1}$ under ambient pressure.

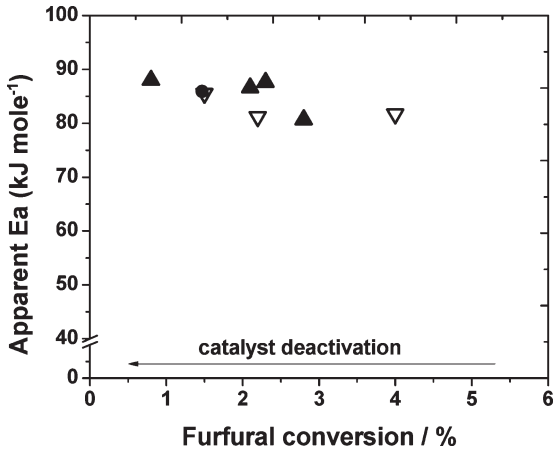

Fig. 9 Apparent activation energy (E_a) as a function of furfural conversion. Different furfural conversions were achieved by using different amounts of Mo_2C catalysts ((●) sample A, (▲) sample B in Table 1, ~0.1–0.64 g) and by catalyst deactivation for the same catalyst (▽, sample A in Table 1) starting from a high furfural conversion of ~4%. E_a was found to be independent of furfural conversion and catalyst deactivation. Experimental data obtained at furfural/CH_4/H_2 = ~0.24%/~2.5%/bal with a total flow rate of ~1.67 $cm^3\ s^{-1}$ under ambient pressure.

section 3.1) were restored upon treating the sample in a flow of H_2 at ~750 K for 1 h (Fig. 4) presumably by removing the carbonaceous species. The observation that the apparent H_2 order is invariant at different furfural conversions, regardless of the change in conversion being achieved by catalyst deactivation or using different catalyst loadings (Fig. 8), reinforces our postulate that it is the number, not the chemistry, of the active sites that is changing during the reaction. The invariance of H_2 order with a furfural conversion ranging from ~0.5% to ~13% also confirms that products of furfural HDO do not have any measurable kinetic effects on 2MF production rates.

The apparent activation energy for vapor phase furfural HDO over Mo_2C catalysts was found to be ~85 kJ mol^{-1} and a typical Arrhenius plot can be found in Fig. S9 in the ESI.† Fig. 9 shows the measured apparent activation energy as a function of furfural conversion, achieved by using different catalyst amounts (0.1–0.64 g) or by deactivation of a catalyst starting from a furfural conversion of ~4%. Similar to the aforementioned conclusion for the apparent H_2 reaction order, the invariant apparent activation energy with furfural conversion confirms that (i) catalyst deactivation is due to a change in the number, not the chemistry, of the active sites and (ii) product inhibition can be neglected under our conditions.

A plausible reaction mechanism, based on experimental observations of an apparent hydrogen order of ~0.5 at a H_2 partial pressure of ~0.1 to ~1 atm and an apparent furfural order between ~0.3 and zero as furfural partial pressure increased from ~0.03 to ~30 kPa and having no kinetic effects of furfural HDO products on the 2MF production rate, is proposed. Hydrogen molecules can adsorb dissociatively on site 1 (S_1) and furfural molecules (R represents a furan ring) are adsorbed on a distinct site 2 (S_2) [eqn (1) and (2)]. The dissociated hydrogen can bind to the oxygen of the adsorbed furfural to give a reaction intermediate (R-CHOH-S_2) [eqn (3)], which might promote C–O bond cleavage on adjacent empty sites, S_2 [eqn (4)]. The adsorbed furfural-derived RCH-S_2 intermediate can then react with dissociated hydrogen sequentially [eqn (5) and (6)] to generate 2MF adsorbed on S_2. The adsorbed 2MF can then desorb [eqn (7)] to complete the catalytic cycle.

$$H_2 + 2S_1 \leftrightarrow 2H\text{–}S_1 \quad (1)$$

$$R\text{–}CHO + S_2 \leftrightarrow R\text{–}CHO\text{–}S_2 \quad (2)$$

$$R\text{–}CHO\text{–}S_2 + H\text{–}S_1 \rightarrow R\text{–}CHOH\text{–}S_2 + S_1 \quad (3)$$

$$R\text{–}CHOH\text{–}S_2 + S_2 \leftrightarrow RCH\text{–}S_2 + HO\text{–}S_2 \quad (4)$$

$$RCH\text{–}S_2 + H\text{–}S_1 \leftrightarrow R\text{–}CH_2\text{–}S_2 + S_1 \quad (5)$$

$$RCH_2\text{–}S_2 + H\text{–}S_1 \leftrightarrow R\text{–}CH_3\text{–}S_2 + S_1 \quad (6)$$

$$R\text{–}CH_3\text{–}S_2 \leftrightarrow R\text{–}CH_3 + S_2 \quad (7)$$

$$HO\text{–}S_2 + H\text{–}S_1 \leftrightarrow H_2O\text{–}S_2 + S_1 \quad (8)$$

$$H_2O\text{–}S_2 \leftrightarrow H_2O + S_2 \quad (9)$$

If we assume that (1) the addition of dissociated hydrogen to the adsorbed furfural intermediate [eqn (3)] is the rate

determining step, which is in line with a recent density functional theory (DFT) calculation result showing that the addition of dissociated hydrogen to a propanal molecule adsorbed on a Mo_2C surface is an energetically demanding step,[20] (2) all other steps are at quasi-equilibrium, and (3) the most abundant reactive intermediate (MARI) for site 1 (S_1) is empty sites and the coverage of the adsorbed furfural intermediate (R-CHO-S_2) is much higher than that for other species on S_2 sites, an equation of 2MF production rate that can account for experimentally observed ~0.5 in H_2 and ~0.3 to zero order in furfural (depending on furfural partial pressure) can be derived (detailed derivation is available in section 3 in the ESI†).

Alternatively, if we assume that the oxygen in furfural can be directly stripped by the carbidic surface due to its oxophilic nature,[20,40,41] the cleavage of the C═O bond in the adsorbed furfural could occur on an adjacent empty site [eqn (10)]. The derived surface-adsorbed furfural fragment (RCH-S_2) and atomic oxygen can react with dissociated hydrogen sequentially to generate adsorbed 2MF [eqn (11) and (12)] and adsorbed water [eqn (14) and (8)], respectively. The adsorbed 2MF and water then can desorb to complete the catalytic cycle [eqn (13)].

$$R\text{–}CHO\text{–}S_2 + S_2 \leftrightarrow RCH\text{–}S_2 + O\text{–}S_2 \quad (10)$$

$$RCH\text{–}S_2 + H\text{–}S_1 \rightarrow R\text{–}CH_2\text{–}S_2 + S_1 \quad (11)$$

$$R\text{–}CH_2\text{–}S_2 + H\text{–}S_1 \leftrightarrow R\text{–}CH_3\ S_2 + S_1 \quad (12)$$

$$R\text{–}CH_3\text{–}S_2 \leftrightarrow R\text{–}CH_3 + S_2 \quad (13)$$

$$O\text{–}S_2 + H\text{–}S_1 \leftrightarrow HO\text{–}S_2 + S_1 \quad (14)$$

Based on the assumptions that (1) the addition of dissociated hydrogen to the furfural intermediate adsorbed on S_2 (RCH-S_2) is the rate determining step [eqn (11)] and (2) empty sites are MARI for S_1 and adsorbed furfural (R-CHO-S_2) has higher coverage than the other species adsorbed on S_2, the same 2MF production rate dependencies with ~0.3 to zero order in furfural (depending on furfural partial pressure) and ~0.5 order in H_2 can be derived (detailed derivation is available in section 3 in the ESI†).

3.4 Site requirements of molybdenum carbide catalysts for vapor phase furfural HDO

Table 2 lists catalysts with varying number of catalytic centers as measured by CO chemisorption at 323 K, which was achieved by using different preparation conditions and/or aging times. We note that except for samples #7 and #8 listed in Table 2, in which both CO chemisorption and kinetic measurements were carried out within two days of the Mo_2C preparation (the catalyst was still passivated and removed from the reactor after synthesis), all other samples were aged in a vial for <1 month. CO chemisorption for samples listed in Table 2, however, was re-measured within 2 days of the kinetics measurement. Considering that sample #7 and samples #3–#6 were prepared using very similar conditions, the significant difference in the CO chemisorption between sample #7 (~200 μmol g^{-1}) and samples #3–#6 (with an average value of ~130 μmol g^{-1}) suggests that ~35% of the catalytic sites, presumably lost due to oxidation, cannot be regenerated by a H_2 flow treatment at ~750 K for 1 h, as discussed in section 3.1 (type A sites categorized by CO chemisorption). This difficulty of removing surface oxygen on a metal carbide surface is in line with the results reported by Ribeiro and coworkers in which only ~50% of surface oxygen on tungsten carbide surfaces can be removed at 1150 K.[42]

The average 2MF STY at 423 K, normalized by the amount of irreversibly chemisorbed CO measured at 323 K, between 2 and 3 h time-on-stream was found to be nearly invariant (~1.2×10^{-4} mol s^{-1} mol_{COsite}^{-1}) for a set of Mo_2C catalysts with varying number of CO chemisorption sites (Table 3). The mechanistic insight from this experimental result is that

Table 3 Catalytic performance (2MF production rate, 2MF turnover rate (TOR), furfural conversion, product selectivity and apparent E_a) of vapor phase furfural HDO for high surface area Mo_2C samples with varying numbers of catalytic centers measured by CO chemisorption at 323 K

Catalyst	CO chemisorption uptake (μmol g^{-1}, STP) at 323 K	2MF production rate[a] (×10^{-9} mol $^{-1}$ s^{-1} g^{-1})	2MF TOR[a] (×10^{-5} mol s^{-1} mol_{COsite}^{-1})	E_a (kJ mol^{-1})	Furfural conversion[a] (%)	Product selectivity[a] (%)		
						2MF	C_{10}^+	Furfuryl alcohol
#1	51	5	10	93.5 ± 3	1.1	37	56	6
#1 (rep)		6	12		1.8	41	53	3
#2	119	17	14		3.3	50	44	4
#3	127	10	8		1.9	45	51	3
#4	135	10	7		2.0	46	48	4
#5	138	21	15		1.0	43	46	8
#6	139	22	16		7.5	60	37	2
#6 (rep)		13	10		2.4	50	45	4
#7	201	23	12		4.2	43	52	3
#8	231	41	18		5.1	54	42	4
#8 (rep)		31	13		3.1	46	47	5

[a] The reported rate represents an average value at 423 K between 1 and 2 h time-on-stream with a furfural conversion of <15%. Reaction conditions: furfural/CH_4/H_2 = ~0.24%/2.5%/bal (total flow rate ~1.67 cm^3 s^{-1}); catalyst loading: 0.036–0.32 g. The CO chemisorption and the kinetic measurements were carried out within 2 days for each sample listed above.

the number of sites assessed by CO chemisorption correlates (whether or not they can be regenerated by H_2 treatment) with the rate of vapor phase furfural HDO on Mo_2C catalysts. The measured average 2MF STY is not a function of the concentration of active sites available, which satisfies the Madon–Boudart criterion confirming the absence of heat and mass transfer limitations.[43]

The composition of transition metal oxides and carbides depends on the gas phase environment, and in the presence of both oxygen containing reactants/products and hydrogen, the possibility of the carbidic surface being oxidized to form an oxycarbide or an oxide, which was not detected by our XRD analysis, cannot be excluded. The requirements of carbidic, oxycarbidic, or oxide phases for HDO chemistry, therefore, remain unknown at this point. Although the structural composition of the two distinct active sites for vapor phase furfural HDO on Mo_2C catalysts cannot be inferred from our results, we report that molybdenum carbide is a very selective catalyst for cleaving the C=O in the furfural with negligible selectivity to C–C bond cleavage products and reveal the site requirements for this chemistry: (1) two distinct sites are required to activate the oxygenate and hydrogen molecules and (2) catalytic rate scales with the number of metallic sites in Mo_2C catalysts measured by *ex situ* CO chemisorption.

Conclusions

Molybdenum carbide catalysts can selectively cleave the C=O bond of the side group of furfural without concurrent C–C bond scission, giving a 2MF selectivity of ~50–60% together with a furan selectivity of <1% at low reaction temperatures of ~423 K under ambient pressure conditions. The negligible fraction of 2-methyltetrahydrofuran indicates that Mo_2C is a very selective hydrodeoxygenation catalyst. Catalyst deactivation, however, was observed and occurred due to a change in the number, not the chemistry and/or identity, of active sites because the measured kinetics, including apparent activation energy (~85 kJ mol^{-1}) and apparent hydrogen order (~0.5), at different furfural conversions (~0.5% to ~13%) were nearly invariant. The products of vapor phase furfural HDO have no measurable kinetic effects on the 2MF production rate. Based on the observed apparent H_2 order (~0.5) and furfural order (~0–0.3), a plausible mechanism consisting of two distinct sites was proposed. Metal-like sites on Mo_2C catalysts were shown to be involved in the furfural HDO reaction *via* the invariance of 2MF STY normalized by the catalytic sites titrated by *ex situ* CO chemisorption.

Acknowledgements

This research was supported by the Catalysis Center for Energy Innovation, an Energy Frontier Research Center funded by the Office of Basic Energy Sciences, U.S. Department of Energy under Award number DE-SC0001004.

References

1 S. Dutta, S. De, B. Saha and M. I. Alam, *Catal. Sci. Technol.*, 2012, **2**, 2025–2036.
2 D. C. Elliott, *Energy Fuels*, 2007, **21**, 1792–1815.
3 G. W. Huber and A. Corma, *Angew. Chem., Int. Ed.*, 2007, **46**, 7184–7201.
4 J. P. Lange, E. van der Heide, J. van Buijtenen and R. Price, *ChemSusChem*, 2012, **5**, 150–166.
5 H. M. Wang, J. Male and Y. Wang, *ACS Catal.*, 2013, **3**, 1047–1070.
6 Y. Nakagawa, M. Tamura and K. Tomishige, *ACS Catal.*, 2013, **3**, 2655–2668.
7 Y. Roman-Leshkov, C. J. Barrett, Z. Y. Liu and J. A. Dumesic, *Nature*, 2007, **447**, 982–U985.
8 V. V. Pushkarev, N. Musselwhite, K. J. An, S. Alayoglu and G. A. Somorjai, *Nano Lett.*, 2012, **12**, 5196–5201.
9 R. Rao, A. Dandekar, R. Baker and M. Vannice, *J. Catal.*, 1997, **171**, 406–419.
10 R. S. Rao, R. T. K. Baker and M. A. Vannice, *Catal. Lett.*, 1999, **60**, 51–57.
11 S. Sitthisa, W. An and D. E. Resasco, *J. Catal.*, 2011, **284**, 90–101.
12 S. Sitthisa, T. Pham, T. Prasomsri, T. Sooknoi, R. G. Mallinson and D. E. Resasco, *J. Catal.*, 2011, **280**, 17–27.
13 S. Sitthisa and D. E. Resasco, *Catal. Lett.*, 2011, **141**, 784–791.
14 S. Sitthisa, T. Sooknoi, Y. G. Ma, P. B. Balbuena and D. E. Resasco, *J. Catal.*, 2010, **277**, 1–13.
15 D. X. Liu, D. Zemlyanov, T. P. Wu, R. J. Lobo-Lapidus, J. A. Dumesic, J. T. Miller and C. L. Marshall, *J. Catal.*, 2013, **299**, 336–345.
16 H.-Y. Zheng, Y.-L. Zhu, L. Huang, Z.-Y. Zeng, H.-J. Wan and Y.-W. Li, *Catal. Commun.*, 2008, **9**, 342–348.
17 R. D. Srivastava and A. K. Guha, *J. Catal.*, 1985, **91**, 254–262.
18 V. Vorotnikov, G. Mpourmpakis and D. G. Vlachos, *ACS Catal.*, 2012, **2**, 2496–2504.
19 W. Zhang, Y. Zhu, S. Niu and Y. Li, *J. Mol. Catal. A: Chem.*, 2011, **335**, 71–81.
20 H. Ren, W. Yu, M. Salciccioli, Y. Chen, Y. Huang, K. Xiong, D. G. Vlachos and J. G. G. Chen, *ChemSusChem*, 2013, **6**, 798–801.
21 W. T. Yu, Z. J. Mellinger, M. A. Barteau and J. G. G. Chen, *J. Phys. Chem. C*, 2012, **116**, 5720–5729.
22 J. X. Han, J. Z. Duan, P. Chen, H. Lou, X. M. Zheng and H. P. Hong, *ChemSusChem*, 2012, **5**, 727–733.
23 R. W. Gosselink, D. R. Stellwagen and J. H. Bitter, *Angew. Chem., Int. Ed.*, 2013, **52**, 5089–5092.
24 A. L. Jongerius, R. W. Gosselink, J. Dijkstra, J. H. Bitter, P. C. A. Bruijnincx and B. M. Weckhuysen, *ChemCatChem*, 2013, **5**, 2964–2972.
25 K. Xiong, W.-S. Lee, A. Bhan and J. G. Chen, *ChemSusChem*, 2014, DOI: 10.1002/cssc.201402033.
26 J. Patt, D. J. Moon, C. Phillips and L. T. Thompson, *Catal. Lett.*, 2000, **65**, 193–195.
27 J. S. Choi, G. Bugli and G. Djega-Mariadassou, *J. Catal.*, 2000, **193**, 238–247.

28 J. S. Lee, S. T. Oyama and M. Boudart, *J. Catal.*, 1987, **106**, 125–133.
29 K. J. Leary, J. N. Michaels and A. M. Stacy, *J. Catal.*, 1986, **101**, 301–313.
30 G. S. Ranhotra, G. W. Haddix, A. T. Bell and J. A. Reimer, *J. Catal.*, 1987, **108**, 24–39.
31 J. Bremner and R. Keeys, *J. Chem. Soc.*, 1947, 1068–1080.
32 M. Choura, N. M. Belgacem and A. Gandini, *Macromolecules*, 1996, **29**, 3839–3850.
33 G. Li, N. Li, Z. Wang, C. Li, A. Wang, X. Wang, Y. Cong and T. Zhang, *ChemSusChem*, 2012, **5**, 1958–1966.
34 A. V. Subrahmanyam, S. Thayumanavan and G. W. Huber, *ChemSusChem*, 2010, **3**, 1158–1161.
35 S. K. Bej, C. A. Bennett and L. T. Thompson, *Appl. Catal., A*, 2003, **250**, 197–208.
36 B. Donnis, R. G. Egeberg, P. Blom and K. G. Knudsen, *Top. Catal.*, 2009, **52**, 229–240.
37 D. Meier, J. Berns, O. Faix, U. Balfanz and W. Baldauf, *Biomass Bioenergy*, 1994, **7**, 99–105.
38 E. I. Ko and R. J. Madix, *Surf. Sci.*, 1980, **100**, L449–L453.
39 E. I. Ko and R. J. Madix, *Surf. Sci.*, 1981, **109**, 221–238.
40 P. Liu and J. A. Rodriguez, *J. Phys. Chem. B*, 2006, **110**, 19418–19425.
41 A. J. Medford, A. Vojvodic, F. Studt, F. Abild-Pedersen and J. K. Norskov, *J. Catal.*, 2012, **290**, 108–117.
42 F. H. Ribeiro, R. A. D. Betta, G. J. Guskey and M. Boudart, *Chem. Mater.*, 1991, **3**, 805–812.
43 R. J. Madon and M. Boudart, *Ind. Eng. Chem. Fundam.*, 1982, **21**, 438–447.

